

1 **Oxygenic phototrophic biofilms for improved cathode** 2 **performance in microbial fuel cells**

3 **X. Alexis Walter^a, John Greenman^a and Ioannis A. Ieropoulos^a**

4 ^a Bristol Robotics Laboratory, Universities of Bristol and of the West of England, T-building, Frenchay Campus,
5 BS16 1QZ, United Kingdom. Fax: +44(0)1173283960;

6 ^b Microbiology Research Laboratory, School of Biomedical Sciences, Faculty of Applied Sciences, Frenchay Campus,
7 University of the West of England, Bristol, BS16 1QY, United Kingdom.

8 Corresponding author: Ioannis A. Ieropoulos / Bristol Robotics Laboratory, Universities of Bristol and of the West of
9 England, T-building, Frenchay Campus, BS16 1QZ, United Kingdom / Tel: +44 (0)117 3286318 / E-mail:
10 ioannis.ieropoulos@brl.ac.uk

11 **Capturing electrons in the cathodic chambers of microbial fuel cells (MFCs) is a typical**
12 **limiting aspect of its performance. Recently, research on biocathodes has gained more**
13 **interest as it allows circumventing the utilisation of exogenous and unstable mediators at**
14 **a lower cost. It is shown here that the growth of oxygenic phototrophs as a biofilm,**
15 **increases the current output by two fold. This was possible by forcing the biofilm to**
16 **grow directly onto the cathode, thus, producing the oxygen directly where it was**
17 **consumed. This enhancement of the cathodic efficiency was stable for over 30 days.**

18 **Key words:** Microbial Fuel Cell, biocathode, oxygenic photosynthesis, biofilm.

19 **1 Introduction**

20 Microbial fuel cells (MFC) are energy transducers comprising an anode and a cathode and
21 typically a cation exchange membrane. In such systems, anaerobic electroactive
22 microorganisms use the anode electrode as an electron acceptor when mineralising organic
23 matter. The resultant electrons pass through an external circuit before arriving at the cathode,
24 where they react with a compound of a higher redox potential (e.g. oxygen, ferricyanide) and
25 cations, thus producing current. The first MFC demonstration was achieved in 1911 [1], but
26 research in the subject has really thrived in the last 20 years and especially this last decade

1 [2], during which a diversity of MFC embodiments, and a variety of parameters depending on
2 the target applications have been demonstrated [3,4]. Recent research has implied the use of
3 phototrophs either as the electron provider for the anode [5,6], or as a potential electron
4 acceptor in the cathodic compartment. In this work we will focus on the use of phototrophs as
5 the catalyst in biocathodes.

6 In conventional MFCs, oxygen reacts with electrons flowing from the cathode, and power
7 outputs are, thus, limited by the high overpotential of oxygen. To overcome this, mediators or
8 catalysts are usually required [7], but with the added problems of increased material costs and
9 hindered sustainability through time. For this reason biocathodes have recently attracted great
10 interest since they can increase power output at a lower cost and with better sustainability
11 [8,9]. The essence of biocathodes is to utilise microorganisms as biocatalysts to mediate the
12 reduction of an oxidant either directly or indirectly [10-12]. One of the numerous possibilities
13 is the use of phototrophs [13].

14 A first study, performed by Cao *et al.*, has shown that anoxygenic phototrophic mixed
15 cultures dominated by *Rhodobacter* and *Rhodospirillum rubrum* (α -Proteobacteria), previously
16 grown on the anodic part of an MFC, were able to accept cathodic electrons and use them for
17 CO₂ carbon fixation in a light dependent manner [14]. As indicated in a recent review, the
18 results of Cao *et al.* do not specifically demonstrate phototrophic microorganisms to be
19 responsible for the electron uptake [12]. In a more recent study, Powell *et al.* have coupled the
20 algal cathodic half-cell (*Chlorella vulgaris*) to a yeast anodic half-cell [15]. They have
21 showed that such an MFC was producing a power density of 0.95 mW.m⁻² at 90 mV, with a
22 load of 5 k Ω . The algae were under agitation and not in direct contact with the cathode, and 2-
23 hydroxy-p-naphthoquinone (HNQ) was used as a mediator. In this study, it was suggested that
24 the electrons from the cathode directly serve the phototrophic organisms to fix CO₂. Since the
25 microorganisms employed were oxygenic phototrophs that were releasing O₂ from the
26 hydrolysis of their electron's source (H₂O), it is difficult to decipher if it was the oxygen
27 present in the catholyte that reacted with the electrons through the mediator, or if it was the

1 phototrophs themselves [15,16], especially since air was pumped into the catholyte
2 “providing oxygen and CO₂” [15]. Nevertheless, it has been shown that *in-situ* phototrophic
3 biofilms formed on an electrode immersed in a river stream, were able to catalyse the oxygen
4 reduction thus, showing that biofilms could be more appropriate than a suspension of
5 planktonic cells, as suggested by Huang *et al.* [17] [10].

6 The aim of the current study was to continue investigations in the field of cathodic efficiency
7 enhancement, with the objective of growing a biofilm of mixed oxygenic phototrophs onto
8 the cathode. The hypothesis is that cathode efficiency can be improved by directly producing
9 the oxygen where it is consumed, thus, avoiding the use of any mediators. This follows from
10 the observation of oxygen-supersaturation in stratified ecosystems, such as in microbial mats,
11 can reach 5-fold higher concentrations [18-20]. The stability of current output was also
12 monitored in order to investigate if such a system could be useful for MFC applications where
13 oxygen is a limiting factor [8,10] (Fig. 1).

14 **2 Material and Methods**

15 **2.1 Strain and culture media**

16 The mixed culture of oxygenic phototrophs used in the cathodic chamber consisted of the
17 cyanobacteria *Synechococcus leopoliensis*, *Anabaena cylindrica* and the algae *Chlorella*
18 *pyrenoidosa* (obtained from “www.sciento.co.uk”). The main reasons for the selection of
19 organisms was to have highly active, fast growing algae and cyanobacteria (*Chlorella*
20 *pyrenoidosa* and *Synechococcus leopoliensis*), but also filamentous cyanobacteria (*Anabaena*
21 *cylindrica*) that would have facilitated the anchoring of the two other strains in the cellulose
22 matrix. All species were grown separately in BG-11 media. A mix culture was obtained by
23 adding 20mL of 10⁸ cells per mL of each parent-culture in the same catholyte reservoirs of 1L
24 prior to its connection to the MFCs. The catholytes consisted of the same BG-11 medium for
25 freshwater strains as the one used for the growth of the oxygenic phototrophs [21]. The
26 anodic compartments were inoculated with a pure culture of *Shewanella oneidensis* MR-1

1 (ATCC- 700550) [22,23]. The *Shewanella oneidensis* cultures were directly introduced into
2 the anodic compartment of the MFC and not the anolyte reservoir. The anolytes consisted of
3 the nutritionally rich LB medium [24].

4 **2.2 MFCs design and operation**

5 The microbial fuel cells were made of acrylic material and comprised two 25mL compartment
6 separated by a cation exchange membrane (CEM) with a 30 cm² surface area (VWR) as
7 described elsewhere [25,26]. The electrodes in both the anode and cathode were a 270 cm²
8 sheet of carbon fibre veil (20 g m⁻²) (PRF Composite Materials Poole, Dorset, UK) folded
9 down to a 3D structure with an exposed surface area of 5 cm². The cathode's side facing the
10 outside was covered by a 5 cm² cellulose matrix (DRY-FRESH 800 NL; Sirane Ltd, Telford,
11 UK) as the substratum for the colonisation by oxygenic phototrophs. However, the cellulosic
12 matrix applied in the *c*MFC had an additional plastic film (high density polyethylene) within
13 interfacial contact with the cellulose sheets, acting as an inhibitor of algal cell attachment. In
14 addition, the *c*MFC differed from the *p*MFC by its anode that had a higher surface area
15 (500cm²). Although the anode surfaces were different, open-circuit voltages (V_o) of the
16 *p*MFC and the *c*MFC could still be compared: V_o reflects the redox potential difference
17 between the two compartments and, thus, is independent of the electrodes surface area [27].
18 Since they had a different anode surface area, the comparison between the current production
19 of the *p*MFC and the *c*MFC (when a load was applied) could only be performed under
20 normalised conditions according to the electrode total macro-surface areas. The
21 photosynthetic MFC (*p*MFC) was inoculated with the culture of oxygenic phototrophs 3
22 weeks after the control MFC (*c*MFC) was inoculated, in order to insure that no oxygenic
23 biofilm was developing on the cathode of the *p*MFC (high density polyethylene film).
24 Both anodic chambers were fed from the same 10L anolyte reservoir, but each MFC had a
25 dripping system in order to isolate the two hydrodynamic circuits thus, avoiding fluidic cross
26 conduction of electrons as well as contamination of the anolyte reservoir(Fig. 2). The anolyte

1 passed through the anodic chamber at a flow of $0.150 \text{ mL min}^{-1}$ and was then discarded
2 (perfusion model [28]). The anolyte was a flow through system, whereas the catholyte was a
3 closed loop system (Fig. 2). In order to force the oxygenic phototrophs to form a true attached
4 biofilm within the cellulose matrix, a high flow of catholyte (24.5 mL min^{-1} instead of 0.15
5 mL min^{-1} for the anolyte) was applied, whilst the 1L reservoir of catholyte was covered with
6 aluminium foil to prevent any algal/bacterial growth (hydraulic retention time (HRT) of 40
7 min). The tubing consisted of black ISO-Versinic (3 mm ID; Saint Gobain Performance
8 Plastics, FR), thus, the only zone open to light was the cathodic chamber (cathodic HRT of 1
9 min). The partial pressure of gas in the catholyte reservoirs was in equilibrium with that of the
10 atmosphere through a sterile air filter of $0.45 \mu\text{m}$ porosity. The MFCs were placed in a light
11 box 50 cm away from a 30W compact fluorescent light bulb (1535 lumens, 6400K daylight)
12 and a 12h dark/light exposure was applied. The temperature was monitored during this
13 experiment and was found to be $27^\circ\text{C} \pm 2^\circ\text{C}$ for both day and night phases.

14 **3 Results and discussion**

15 After 30 days, only a small proportion of the *c*MFC's cathode surface was colonised whereas
16 the *p*MFC cellulose sheet was entirely covered by an oxygenic phototrophic biofilm (by
17 visual inspection). This allowed the comparison of the impact of a cathodic biofilm of
18 oxygenic phototrophs on the MFC performance, in which case only the *p*MFC had developed
19 an oxygenic phototrophic biofilm onto its cathode. Open circuit voltages (V_{O}) measured
20 during the first 14 days of the experiment indicated that only the *p*MFC developed a light-
21 dependent behaviour (Fig. 3a). This light response became noticeable 5 days after the
22 reservoir inoculation by the mixture of oxygenic phototrophs (OP) and stabilised after the 6th
23 day. On the contrary, the V_{O} measured in the *c*MFC, did not indicate any light response:
24 $540.75 \pm 6.61 \text{ mV}$ between day 5 and day 15. In fact, the V_{O} measured in *c*MFC, under either
25 light or dark treatment, corresponded to the V_{O} measured during the dark phases of *p*MFC
26 (Fig. 1a). During the same period, the daylight V_{O} reached a plateau (*p*MFC), which was

1 always $25 \text{ mV} \pm 2.27 \text{ mV}$ higher than the night-time one. As those day light V_O variations
2 were light-dependent, they were probably influenced by the activity of the photosynthetic
3 organisms. Since the only phototrophic microorganisms present were the ones performing
4 oxygenic photosynthesis, it can be thus assumed that during the light phase oxygen was
5 produced. In a MFC, open circuit voltage is a reflection of the redox potential between the
6 two half-cells. The fact that the V_O increased during the light phase, suggests that this was the
7 result of a strong oxidant being produced in the cathodic compartment rather than a reducing
8 agent produced in the anode compartment.

9 A $7.5 \text{ k}\Omega$ load was applied to both *p*MFC and *c*MFC on the 14th day of the experiment (Fig.
10 3b). Results confirmed that the same light response was observed under current production
11 (Fig. 3b). The loaded circuit voltage (V_L) was characterised by a similar pattern between the
12 day steady-state and the night one. However, the differences between those two steady-states
13 increased 6 days after the application of the load. Then, starting from the 7th day, the system
14 stabilised in V_L between night and day steady-states ($\delta V_{\text{day/night}}$) (Fig. 3b). The standard
15 deviation of V_L average values (Tab. 1) shows that the system was very stable during each
16 steady-state. Moreover, in comparison to V_O , the V_L was characterised by a higher $\delta V_{\text{day/night}}$
17 ($75.8 \text{ mV} \pm 7.8 \text{ mV}$). Those day-to-day variations were also stable as diurnal oscillations until
18 the end of the experiments, thus, showing consistency through time.

19 The methodology and results published by Powell *et al.* being the closest to the present study
20 and containing the appropriate information, allowed a valid comparison [15]. They reported,
21 for the maximum power density, a voltage of 90 mV with a $5 \text{ k}\Omega$ resistance that corresponds
22 to $18 \text{ }\mu\text{A}$ and $1.62 \text{ }\mu\text{W}$. In the present study, the highest voltage measured was 157 mV with a
23 load of $7.5 \text{ k}\Omega$. However, no polarisation data had been produced and such a load should not
24 allow maximum power transfer. Nevertheless, these findings correspond to a current of 20.9
25 μA , calculated using Ohm's law ($I = V_L/R$), and a power (P) of $3.29 \text{ }\mu\text{W}$ ($P = I \times U$) (Tab. 2).
26 Thus, the values obtained are in the same range as in the Powell *et al.* study or as reported for

1 a nitrate-based biocathode [15,29]. In order to give values that could be compared, we
2 calculated the current density normalised either on the **Total Macroscopic Surface Area**
3 (**TMSA**, correspond to the unfolded surface area of the anode) or on the **Projected Surface**
4 **Area (PSA**, corresponding to the geometric surface area of the folded anode) (Tab. 2). As
5 shown, the values vary considerably and are obviously 53 fold higher when using the PSA.
6 Because the anodic microorganisms used the anode in direct contact to transfer their electrons
7 [23], the TMSA is more representative in terms of power output for a mediator-less MFC
8 [30]. The PSA remains pertinent in regard to the surface footprint occupied by the whole
9 MFC apparatus for practical application purposes.

10 As the system was stable over the final 9 days of the experiment, the V_L values of each time
11 point were averaged and superimposed in order to represent a 24 h cycle characterising the
12 *p*MFC and *c*MFC, with voltage measurements taken every two minutes (720 pts per day). In
13 this instance, each day is considered as a replicate that reflects day to day variations. Then,
14 using Ohm's law, the current density of a representative 24 h cycle was calculated (Fig. 3c).
15 The current density of the *c*MFC, during both the light and dark phases, corresponded to the
16 dark phase of the *p*MFC (Fig. 3c), thus, confirming a positive increase of current by the
17 oxygenic biofilm. The positive increase of current production in response to illumination was
18 relatively fast (Fig. 3c): in 67 min 90 % of the day steady-state current output increase was
19 reached, with 50 % the first 18 min \pm 1 min. However, it took 6h30 for the light steady-state
20 to be reached (Fig. 3c).

21 **4 Conclusions**

22 In summary, the results presented in the current study confirmed that i) the presence of an
23 oxygenic biofilm enhanced the current produced by the *p*MFC only upon illumination, and ii)
24 this effect was stable over time. These results suggest that the enhancement of the MFC
25 power output by the presence of an oxygenic biofilm could be due to the oxygen
26 supersaturation effect always observed in stratified ecosystems [18-20] (Fig. 4). Future

1 development of biocathodes based on oxygenic biofilm would imply deeper investigations
2 like oxygen micro-profiling into the biofilm in order to confirm if this enhancement is due to
3 an oxygen supersaturation effect or not.

4 **Acknowledgments**

5 This work is funded by the EPSRC under the grant no. EP-H046305-1. Dr. Ioannis Ieropoulos
6 is funded by the EPSRC Career Acceleration Fellowship, Grant no. EP/I004653/1

8 **Notes and references**

9 ^a *Microbiology Research Laboratory, School of Biomedical Sciences, Faculty of Applied*
10 *Sciences, Frenchay Campus, University of the West of England, Bristol, BS16 1QY, United*
11 *Kingdom.*

12 ^b *Bristol Robotics Laboratory, Universities of Bristol and of the West of England, T-building,*
13 *Frenchay Campus, BS16 1QZ, United Kingdom. Fax: +44(0)1173283960; Tel: +44 (0)117*
14 *3286788; E-mail: xavier.walter@uwe.ac.uk*

- 15 [1] M. C. Potter, Electrical Effects Accompanying the Decomposition of Organic Compounds, Proceedings of The Royal Society B 84
16 (1911) 260-276.
- 17 [2] D. Pant, G. Van Bogaert, L. Diels and K. Vanbroekhoven, A review of the substrates used in microbial fuel cells (MFCs) for sustainable
18 energy production, *Bioresource Technol* 101 (2010) 1533-1543.
- 19 [3] B. E. Logan, B. Hamelers, R. A. Rozendal, U. Schröder, J. Keller, S. Freguia, P. Aelterman, W. Verstraete and K. Rabaey, Microbial
20 fuel cells: Methodology and technology, *Environ Sci Technol* 40 (2006) 5181-5192.
- 21 [4] Z. W. Du, H. R. Li and T. Y. Gu, A state of the art review on microbial fuel cells: A promising technology for wastewater treatment and
22 bioenergy, *Biotechnol Adv* 25 (2007) 464-482.
- 23 [5] M. Rosenbaum, U. Schröder and F. Scholz, Utilizing the green alga *Chlamydomonas reinhardtii* for microbial electricity generation: a
24 living solar cell, *Appl Microbiol Biot* 68 (2005) 753-756.
- 25 [6] J. M. Pisciotta, Y. Zou and I. V. Baskakov, Light-Dependent Electrogenic Activity of Cyanobacteria, *Plos One* 5 (2010)
- 26 [7] S. Oh, B. Min and B. E. Logan, Cathode performance as a factor in electricity generation in microbial fuel cells, *Environ Sci Technol* 38
27 (2004) 4900-4904.
- 28 [8] Z. He and L. T. Angenent, Application of bacterial biocathodes in microbial fuel cells, *Electroanal* 18 (2006) 2009-2015.
- 29 [9] A. Ter Heijne, D. P. B. T. B. Strik, H. V. M. Hamelers and C. J. N. Buisman, Cathode Potential and Mass Transfer Determine
30 Performance of Oxygen Reducing Biocathodes in Microbial Fuel Cells, *Environ Sci Technol* 44 (2010) 7151-7156.
- 31 [10] L. P. Huang, J. M. Regan and X. Quan, Electron transfer mechanisms, new applications, and performance of biocathode microbial fuel
32 cells, *Bioresource Technol* 102 (2011) 316-323.
- 33 [11] D. R. Lovley, Powering microbes with electricity: direct electron transfer from electrodes to microbes, *Env Microbiol Rep* 3 (2011) 27-
34 35.
- 35 [12] M. Rosenbaum, F. Aulenta, M. Villano and L. T. Angenent, Cathodes as electron donors for microbial metabolism: Which extracellular
36 electron transfer mechanisms are involved?, *Bioresource Technol* 102 (2011) 324-333.
- 37 [13] M. Rosenbaum, Z. He and L. T. Angenent, Light energy to bioelectricity: photosynthetic microbial fuel cells, *Curr Opin Biotech* 21
38 (2010) 259-264.
- 39 [14] X. X. Cao, X. Huang, P. Liang, N. Boon, M. Z. Fan, L. Zhang and X. Y. Zhang, A completely anoxic microbial fuel cell using a photo-
40 biocathode for cathodic carbon dioxide reduction, *Energ Environ Sci* 2 (2009) 498-501.

- 1 [15] E. E. Powell, R. W. Evitts, G. A. Hill and J. C. Bolster, A Microbial Fuel Cell with a Photosynthetic Microalgae Cathodic Half Cell
2 Coupled to a Yeast Anodic Half Cell, *Energ Source Part A* 33 (2011) 440-448.
- 3 [16] E. E. Powell, M. L. Mapiour, R. W. Evitts and G. A. Hill, Growth kinetics of *Chlorella vulgaris* and its use as a cathodic half cell,
4 *Bioresource Technol* 100 (2009) 269-274.
- 5 [17] E. Lyautey, A. Courmet, S. Morin, S. Bouletreau, L. Etcheverry, J. Y. Charcosset, F. Delmas, A. Bergel and F. Garabetian,
6 Electroactivity of Phototrophic River Biofilms and Constitutive Cultivable Bacteria, *Appl Environ Microb* 77 (2011) 5394-5401.
- 7 [18] N. P. Revsbech, B. B. Jorgensen, T. H. Blackburn and Y. Cohen, Microelectrode Studies of the Photosynthesis and O₂, H₂S, and Ph
8 Profiles of a Microbial Mat, *Limnol Oceanogr* 28 (1983) 1062-1074.
- 9 [19] X. A. Walter, Diversité bactérienne et biogéochimique de tapis microbiens d'eau douce dans la tourbière de Cadagno, MSc thesis,
10 University of Neuchâtel, Switzerland, 2006.
- 11 [20] C. Dupraz, R. P. Reid, O. Braissant, A. W. Decho, R. S. Norman and P. T. Visscher, Processes of carbonate precipitation in modern
12 microbial mats, *Earth-Science Reviews* 96 (2009) 141-162.
- 13 [21] R. Rippka, J. Deruelles, J. B. Waterbury, M. Herdman and R. Y. Stanier, Generic assignments, strain histories and properties of pure
14 cultures of cyanobacteria, *J Gen Microbiol* 111 (1979) 1-61.
- 15 [22] B. E. Logan, Exoelectrogenic bacteria that power microbial fuel cells, *Nat Rev Microbiol* 7 (2009) 375-381.
- 16 [23] Y. A. Gorby, S. Yanina, J. S. McLean, K. M. Rosso, D. Moyles, A. Dohnalkova, T. J. Beveridge, I. S. Chang, B. H. Kim, K. S. Kim, D.
17 E. Culley, S. B. Reed, M. F. Romine, D. A. Saffarini, E. A. Hill, L. Shi, D. A. Elias, D. W. Kennedy, G. Pinchuk, K. Watanabe, S. Ishii, B.
18 Logan, K. H. Nealson and J. K. Fredrickson, Electrically conductive bacterial nanowires produced by *Shewanella oneidensis* strain MR-1
19 and other microorganisms (vol 103, pg 11358, 2006), *P Natl Acad Sci USA* 106 (2009) 9535-9535.
- 20 [24] Y. F. Yang, D. P. Harris, F. Luo, W. L. Xiong, M. Joachimiak, L. Y. Wu, P. Dehal, J. Jacobsen, Z. M. Yang, A. V. Palumbo, A. P.
21 Arkin and J. Z. Zhou, Snapshot of iron response in *Shewanella oneidensis* by gene network reconstruction, *Bmc Genomics* 10 (2009)
- 22 [25] H. P. Bennetto, Electricity generation by microorganisms, *Biotechnology education* 1 (1990) 163-168.
- 23 [26] I. A. Ieropoulos, J. Greenman, C. Melhuish and J. Hart, Comparative study of three types of microbial fuel cell, *Enzyme Microb Tech*
24 37 (2005) 238-245.
- 25 [27] G. C. Gil, I. S. Chang, B. H. Kim, M. Kim, J. K. Jang, H. S. Park and H. J. Kim, Operational parameters affecting the performance of a
26 mediator-less microbial fuel cell, *Biosens Bioelectron* 18 (2003) 327-334.
- 27 [28] J. Greenman, C. McKenzie, S. Saad, B. Wiegand and J. C. Zguris, Effects of chlorhexidine on a tongue-flora microcosm and VSC
28 production using an in vitro biofilm perfusion model, *J Breath Res* 2 (2008)
- 29 [29] Y. H. Jia, H. T. Tran, D. H. Kim, S. J. Oh, D. H. Park, R. H. Zhang and D. H. Ahn, Simultaneous organics removal and bio-
30 electrochemical denitrification in microbial fuel cells, *Bioproc Biosyst Eng* 31 (2008) 315-321.
- 31 [30] I. A. Ieropoulos, J. Winfield, J. Greenman and C. Melhuish, Small Scale Microbial Fuel Cells and Different Ways of Reporting Output,
32 *Electrochemical Society Transaction* 28 (2010) 1-9.
- 33
34

1 **Tab. 1:** Differences between day and night V_L plateaus of the p MFC. The hours in
2 parentheses indicate the period covered by the average calculations. The standard deviation
3 (STDV) accounts for all the points (1 every 2 min) of the period covered by the voltage
4 average. The averaged STDV accounts for the 9 days (day 22 to 30).

5

Day	Night Voltage average (00:01 to 05:41) (mV)	STDV (mV)	Day Voltage average (14:01 to 18:05) (mV)	STDV (mV)	Day/Night difference (mV)
22	85.540	0.553	152.179	0.627	66.639
23	82.446	0.401	143.911	2.914	61.466
24	77.724	0.832	154.233	1.265	76.509
25	77.464	1.064	153.975	0.632	76.511
26	79.413	0.661	158.974	0.662	79.561
27	80.136	0.780	169.312	1.469	89.176
28	87.557	0.341	163.103	0.474	75.546
29	81.660	0.219	160.293	0.428	78.633
30	80.025	0.529	158.045	0.598	78.020
Average	81.330	3.402	157.114	7.210	75.784

6

7

1

2 **Tab. 2:** The highest current and power density values, of the *p*MFC, normalise either by the
3 **Total Macroscopic Surface Area (TMSA)** or by the **Projected Surface Area (PSA)**. The day
4 voltage plateau was 157 mV with a load of 7.5 K Ω . The electrodes surfaces were of 270 cm²
5 (TMSA: total macroscopic surface area) or 5 cm² (PSA: projected surface area).

6

	Absolute	TMSA (m⁻²)	PSA (m⁻²)
Current (mA)	0.0210	0.775	41.866
Power (mW)	0.0033	0.122	6.580

7

8

1

2 **Figure captions**

3 **Fig. 1: Diagram of a microbial fuel cell.** During organic matter mineralisation, the electron
4 is transfer by the biofilm (*Shewanella oneidensis*) to the anode. Electrons flow through an
5 external circuit and protons flow through the membrane. The protons then react with the
6 electrons at the cathode and reduce oxygen into water. In this work, the oxygen is provided by
7 the oxygenic phototrophic biofilm that grow directly on the cathode.

8

9 **Fig. 2: Microbial fuel cell experimental setup.** This diagram illustrates the recycled flow of
10 catholyte and the passing through of the anolyte. The anodic compartment is separated from
11 the reservoir of anolyte, by a dripping system, to prevent any contamination. Each MFC had
12 its own catholyte reservoir. As both MFCs have the same anolyte reservoir, they have their
13 own dripping system.

14

15 **Fig. 3: Voltage and power curve of the setup.** a) Open circuit voltage of the MFCs. The
16 *c*MFC (inoculated with oxygenic microorganisms but without any biofilm. The minor
17 variations observed for the *c*MFC are due to the diurnal temperature cycle. The *p*MFC
18 (containing a cathodic oxygenic biofilm comprising of *Synechococcus leopoliensis*,
19 *Anabaena cylindrica* and *Chlorella pyrenoidosa*) voltage clearly demonstrates a light
20 dependant response. b) Loaded circuit voltage (7.5k Ω) showing the positive light response of
21 the *p*MFC and the stability over time of its current production. c) Current density of the
22 *p*MFC and the *c*MFC over an average 24h diurnal cycle, calculated by the superimposed
23 current measured from day 21 to day 30 (load of 7.5k Ω), where the cathodic oxygenic
24 phototrophic biofilm current increase during light phase is clearly shown.

25

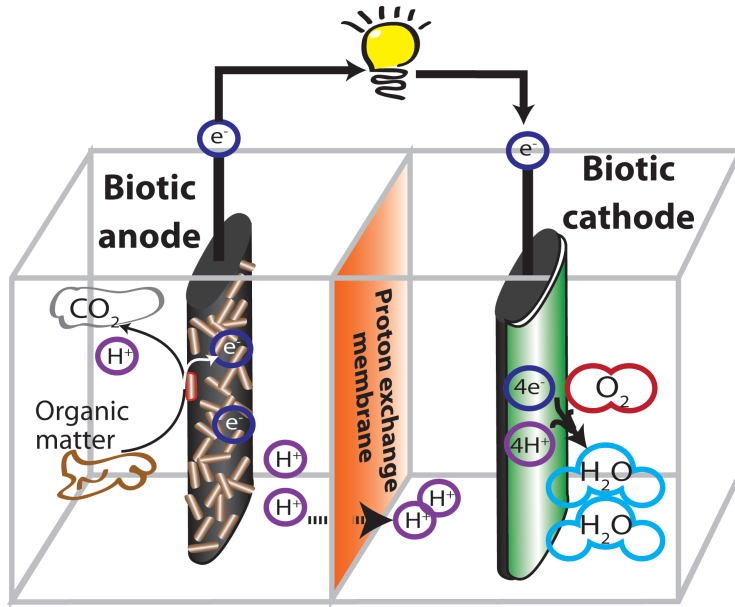
26 **Fig. 4: Local oxygen supersaturation.** This diagram illustrates the suggested principle

1 behind the light-dependent current increase: when in steady-state conditions, because of an
2 oxygen diffusion limitation caused by the oxygenic biofilm, as in microbial mats, a zone of
3 high oxygen concentration appears within the biofilm. As the biofilm covers the cathode, a
4 higher oxygen concentration is available for accepting incoming electrons.

5

6

1



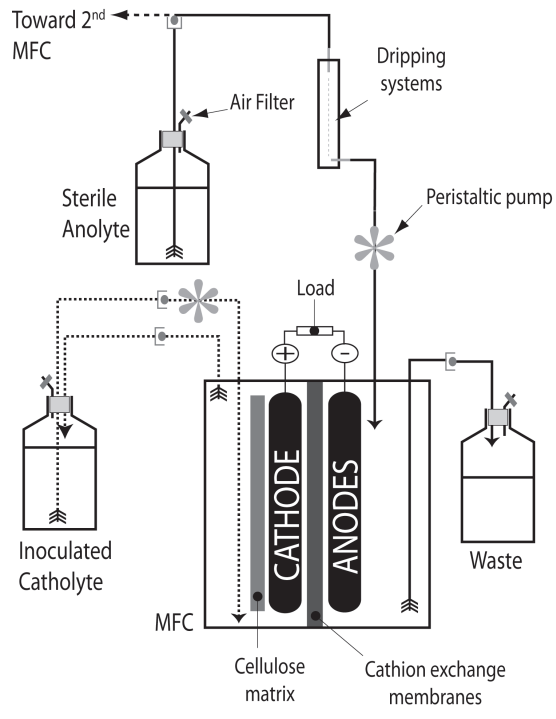
2

3

4

Figure 1

1



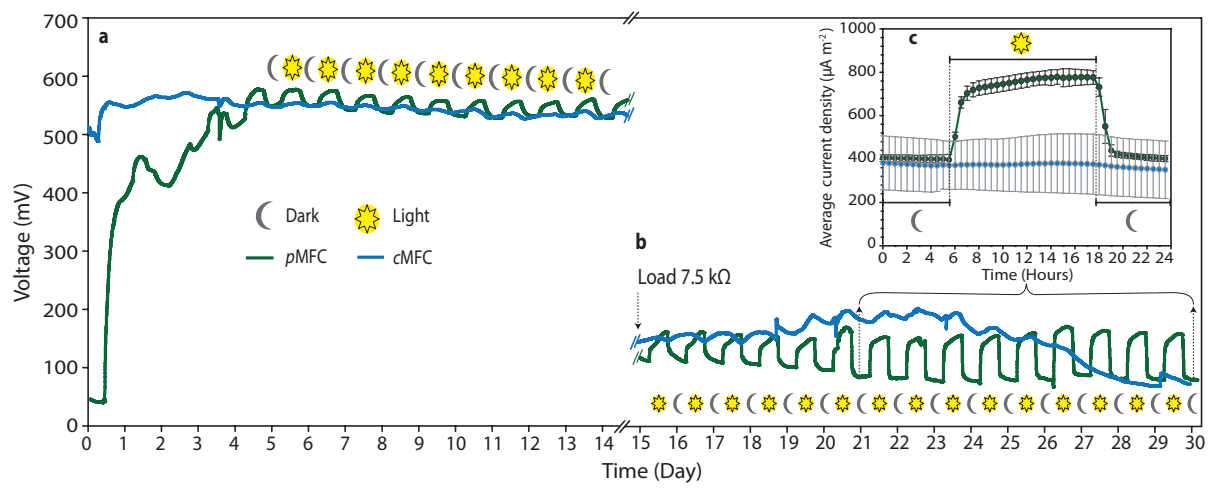
2

3

4

Figure 2

1



2

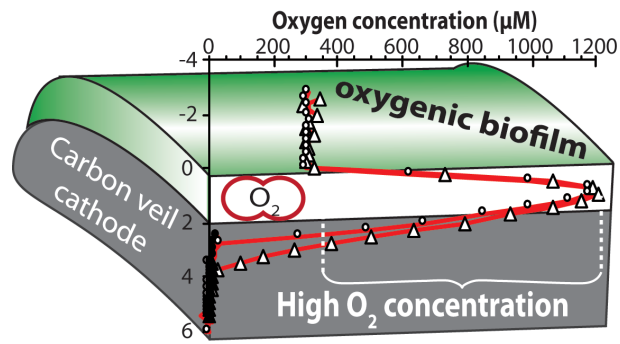
3

4

Figure 3

5

1



2

3

4

Figure 4